Polym. Bull. (2012) 68:693–703
DOI 10.1007/s00289-011-0572-2

ORIGINAL PAPER

# L-Lysine derived novel optically active poly (ester-imide)/clay nanocomposites: study on synthesis and characterization

**Saeed Zahmatkesh**

Received: 26 May 2011 / Revised: 30 June 2011 / Accepted: 30 June 2011 /
Published online: 13 July 2011


**Abstract** A new optically active poly(ester-imide) (PEI) was synthesized from the interfacial polymerization of Ethyl L-lysine-N,N′-ditrimellitoyl diacyl chloride with bis phenol A. Ultrasonic irradiation was applied to compose nanocomposites from the synthetic polymer and different ratios of organo-modified montmorillonite (MMT). The formation of PEI was confirmed by $^{1}$H NMR, FT–IR spectroscopy, specific rotation, and elemental analysis. The resulting nanocomposites were characterized by FT–IR, powder X-ray diffraction (XRD), transmission electron microscopy (TEM), and thermogravimetric analysis (TGA). The results indicated that the composites were dispersed homogeneously in PEI matrix on nanoscale. An improvement in heat stability is indicated from TGA analysis.

**Keywords** Chiral · Nanocomposite · Synthesis · Amino acid · Polyimide

## Introduction

Chiral polymers have attracted a large deal of interest in drug delivery, tissue engineering, dentistry, and chiral stationary phases for resolution of enantiomers in chromatographic techniques because of their promising properties [1]. L-Lysine in particular has been repeatedly used for making polyamides with potential as biomaterials [2]. Poly(ester-imide)s (PEI)s containing heterocyclic imide structures along the main chain of the polymer backbone are used as high-performance engineering resins [3]. The major draw back of them is the disadvantageous properties of these materials, such as poor mechanical properties, high hydrophilicity, and poor processibility, which limit their application. Taking this situation

S. Zahmatkesh (✉)
Department of Science, Payame Noor University, 19395-4697 Tehran, Islamic Republic of Iran
e-mail: zahmatkesh1355@yahoo.com

into consideration, we can easily understand the necessity and the urgency of functionalization and modification to these polymers.

In recent decades, nanotechnology has been widely applied to polymeric materials, with the ultimate goal of dramatically enhanced performance [4, 5]. The applications of inorganic particles in organic composite material became imperative since reduction in dimensions of the particles results in the manifestation of a new crystal motif, or conceivably a new physical phenomenon that does not exist in materials with larger particle sizes [6]. Bionanocomposites can symbolize a novel group of composite biomaterials for tissue engineering and biomedical implants and devices.

The most common inorganic particles belong to the family of 2:1 phyllosilicates. Their crystal structure consists of aluminium or magnesium hydroxide octahedral sheet sandwiched between two silicon oxide tetrahedral sheets. The layer thickness of each platelet is around 1 nm, and their lateral dimensions may vary from 30 nm to several microns [7]. Along with the clay minerals montmorillonite (MMT) is the most studied because of its favorable characteristics, such as swelling ability and cationic exchange capacity [8]. In the synthesis of polymer clay nanocomposites, the clay is treated with an organic modifier before it is mixed with the polymer [7].

Several technologically important polycondensations have been used in nanocomposites preparation with layered silicate such as poly(ethylene terephthalate) [9] polyimides [10], poly(amic acid) [11].

Ultrasonic irradiation is one of the best routs to distribute the nano-sized particles in a polymer matrix in order to prepare nanocomposites [12]. This rout can control the size distribution and morphology of the nano-sized particles, for example poly(dimethylsiloxane)/MMT nanocomposites were synthesized by sonicating a mixture of silanolterminated poly(dimethylsiloxane) (PDMS) and a commercial organosilicate at room temperature for 2 min [13].

In this study, a novel optically active PEI with good thermal stability, optical activity as well as good solubility in common organic solvents which is based on L-lysine is prepared. Then the optically active poly(ester-imide)/organo-modified montmorillonite (MMT) nanocomposites were synthesized under ultrasonic irradiation. The resulting nanocomposites are characterized by various techniques including FT–IR, XRD, TGA, and their morphology were investigated by TEM analyses. The major importance of these nano composites is their optical activity which is based on the natural L-alanine so they can potentially be considered to design the artificial organs.

## Experimental

### Materials and instruments

All chemicals were purchased from Fluka and Merck Chemical Co. Cloisite $Na^+$ with a cation exchange capacity (CEC) of 95 meq/100 g was obtained from Southern Clay Products Inc., Texas, USA.

Proton nuclear magnetic resonance ($^1$H NMR, 500 MHz) spectra were carried out at a Bruker Advance (Germany) 500 instrument. FT–IR spectra were recorded

on a Bruker FT–IR spectrophotometer. UV spectra were recorded on a Perkin-Elmer lambada 5 spectrophotometer. Inherent viscosity was measured by using a Cannon–Fenske Routine Viscometer (Germany) at the concentration of 0.5 g/dL at 25 °C. Specific rotations were measured by a A. Kruss Optronic P3002 RS (Germany) Polarimeter. Thermal gravimetric analysis (TGA) data for polymers were taken on a STA503 WinTA instrument in a nitrogen atmosphere at a rate of 10 °C/min. DSC analyses were preformed on a Mettler DSC-30 under nitrogen atmosphere in a nitrogen atmosphere at a rate of 10 °C/min. Elemental analyses were performed by CHNS-RAPID Heraeus. The XRD patterns of the polymer and nanocomposites were recorded using a Bruker D8 Advance. The analyses were carried out with a scanning rate of 2°/min with Cu Kα radiation ($\lambda = 1.5401$ Å) at a generator voltage of 40 kV and current of 100 mA. The range of the diffraction angle was $2\theta = 3°$–$23°$. The basal spacing was analyzed by Bragg's equation ($d = \lambda/2\sin\theta$). Transmission electron microscopy (TEM) analyses were performed using a Hitachi TM-100 with an accelerating voltage of 80 kV. The reaction was carried out on MISONIX ultrasonic liquid processor, XL-2000 SERIES.

## Monomer synthesis

Synthesis of ethyl L-lysine dihydrochloride [4]

According to the reported article; using EtOH as starting material. Yield: 87%; m.p.: 136–137 °C; IR ($cm^{-1}$): 3421, 3350–2514, 2019, 1740, 1603, 1583, 1501, 1217, 851, 740; $^1$H NMR ($D_2O$, ppm): 1.07 (3H, t, 7 Hz), 1.29 (2H, br), 1.49 (2H, br), 1.76 (2H, br), 2.78 (2H, br), 3.91 (1H, t, 4.3 Hz), 4.08 (2H, br); Elemental analysis for $C_8H_{18}N_2O_2{\cdot}2HCl$, Calcd. C (38.87%), H (8.16%), N (11.33%), Found: C (38.62%), H (8.31%), N (11.40%).

Synthesis of ethyl L-lysine-N,N′-ditrimellitoyl diacide (**1**)

Into a 25 mL round-bottomed flask, 2.000 g ($10.42 \times 10^{-3}$ mol) of trimellitic anhydride, 1.282 g ($5.21 \times 10^{-3}$ mol) of ethyl L-lysine dihydrochloride, a mixture of acetic acid/pyridine (5 mL, 3:2) and a stirring bar were placed. The mixture was stirred at r.t. for 2 h and then refluxed for 6 h. The solvent were removed under reduced pressure. 5 mL of cold concentrated HCl was added. A white precipitate was formed and filtered off. The white diacid (**1**) was extracted from this crude product with chloroform. Yield: 2.32 g (79%); mp: 168 °C; $[\alpha]_D^{25} = +3.14^o$ (0.050 g in 10 mL DMF); IR ($cm^{-1}$): 3400–2400, 1702, 1498, 1418, 1296, 1148, 1069, 1018, 916, 803, 750, 748; $^1$H NMR (500 MHz, $CDCl_3$): $\delta$ 1.2 (3H, t, 7.06 Hz), 1.3 (2H, br), 1.7 (1H, br), 1.8 (1H, br), 2.1 (1H, br), 2.2 (1H, br), 3.7 (2H, t, 4.1 Hz), 4.2 (2H, q, 3.9 Hz), 4.8 (1H, t, 4 Hz), 7.9 (1H, s), 8.0 (1H, s), 8.1 (1H, s), 8.2 (1H, s), 8.4 (1H, s), 8.5 (1H, s), 10.2 (2H, s); $^{13}$C NMR (125 MHz, $CDCl_3$): $\delta$ 14.4, 23.6, 27.7, 28.2, 38.0, 52.4, 62.5, 123.8, 124.1, 124.8, 125.2, 132.2, 132.4, 134.9, 135.1, 136.2, 136.4, 136.5, 136.6, 166.8, 166.9, 167.6, 167.7, 169.3, 170.1, 170.2.

Synthesis of ethyl L-lysine-N,N′-ditrimellitoyl diacylchloride (**2**)

According to the reported article [14]; yield: 0.486 g (82%) of white crystals. dp: 175 °C; $[\alpha]_D^{25} = +4.08^o$ (0.050 g in 10 mL DMF); IR (KBr, $cm^{-1}$): 3023, 2784, 1862, 1785, 1720, 1464, 1384, 1226, 1017, 922, 877, 754, 718, 680, 507.

## Preparation of poly(ester-imide)

Into a 25 mL round-bottomed flask in an ice bath, 1 mmol of ethyl L-lysine-N,N′-ditrimellitoyl diacylchloride (**2**), 7 mL of dichloromethane and a stirring bar were placed. A solution of bis phenol A (1 mmol) in water (10 mL), sodium hydroxide (6.3 mL, 0.1 N) and catalytic amount of tetraethylammonium bromide was prepared. This solution was added dropwise to the flask during 10 min with stirring the mixture vigorously. After stirring for 3 h, the polymer was filtered of, washed with methanol and vacuum dried. Yield: 85%; $\acute{\eta}_{inh}$ (dl $g^{-1}$): 0.34; UV ($\lambda_{max}$, nm) in DMF: 260.87; $[\alpha]_D^{25} = +27.20°$ (0.050 g in 10 mL DMF); IR ($cm^{-1}$): 3461, 2966, 1718, 1614, 1507, 1387, 1282, 1247, 1205, 1173, 1099, 1017, 833, 727, 557; $^1$H NMR (500 MHz, $CDCl_3$): $\delta$ 1.1 (3H, br), 1. 2 (2H, br), 1.5 (2H, br), 1.6 (6H, br), 2.1 (2H, br), 3.5 (2H, br), 4.1 (2H, br), 4.8 (1H, br), 6.6 (2H, br), 6.9–7.0 (2H, br), 7.2 (2H, br), 7.3 (2H, br), 8.0 (1H, br), 8.2 (1H, br), 8.3 (1H, br), 8.5 (1H, br), 9.1 (1H, br), 9.2 (1H, br); $T_{10\%}$: 322; $T_g$: 112.65.

## Preparation of organo-modified Cloisite $Na^+$ [15]

The organo-modified montmorillonite (MMT) was prepared by a cation-exchange method, which is a displacement of the sodium cations of Cloisite $Na^+$ with the protonated dodecyl amine in DMAc/$H_2O$ (50%). The montmorillonite (1.0 g, 0.95 meq) was dispersed in 200 mL of DMAc/deionized water (50%). The amount of protonated dodecyl amine added was about 1 CEC, based on the cation exchange capacity (CEC = 0.95 meq/100 g) of the MMT. This dispersion was mixed and stirred vigorously at 70 °C for 5 h, followed by filtration and continuous washing at 70 °C with deionized water until no chloride ions were detected using an aqueous silver nitrate (AgNO3) solution. The solvent was removed by evaporation under vacuum. The modified montmorillonite was then dried for 12 h, at 70 °C.

## Preparation of poly(ester-imide)/clay bionanocomposites organo-modified Cloisite $Na^+$

Different amounts of prepared 12$CH_3$-MMT (5, 10, 20 wt%) were first swollen in DMAc. Then the layered silicate dispersion mixed with the solution of PEI and the mixture was stirred at 70 °C for 5 h and then irradiated under ultrasound waves (power of 70 W at 72 kHz) for 6 h and precipitated in deionized water.

Characterization was carried out for the solid residues collected via a centrifuge. The solids were washed with water and were vacuum dried at 70 °C for 6 h.

## Results and discussion

The chemical structure of diacid **1** was confirmed by spectroscopic analysis (Scheme 1, Fig. 1). High speed and high yield are the advantages of this polymerization method (Scheme 2).

The wetting property of organo-silicates ($12CH_3$-MMT) is increased due to alkyl ammonium cations. Preparation of PEI/$12CH_3$-MMT nanocomposites was performed by an ultrasonic irradiation technique. Commonly, the main effects of sonication are because of the growth and explosive disintegration of microscopic bubbles on a microsecond time scale. This can generate a rigorous environment of local temperature up to 5000 K and local pressure up to 500 atm. $12CH_3$-MMT which has polar groups could be dispersed completely in polymer matrix via different interactions with the functional groups of the obtained PEI. Although the resulting PEI has lots of polar groups such as carbonyl and nitrogen but with respect to these functional groups they are not much difference between FT–IR spectra of resulting nonocomposites with that of pure PEI except for the Si–O, Al–O, and Mg–O bands which proves the presence of MMT in the PEI matrix. As a result the polymer and $12CH_3$-MMT are exfolicated somewhat, this can be observed from the photograph of TEM. FT–IR spectra of pure MMT (a), $12CH_3$-MMT (b), pure PEI (c), and PEI/$12CH_3$-MMT (5 wt%) (d) are represented in Fig. 2. In pure MMT, OH stretching and bending bands are observed at 3624 and 1630 $cm^{-1}$, respectively. A broad absorption peak at 1040 $cm^{-1}$ is assigned to the Si–O stretching band. In the case of $12CH_3$-MMT, The peak at 2865–2921 $cm^{-1}$ is attributed to CH stretching band of dodecyl group, which are not observed in pure MMT. The FT–IR spectrum of pure PEI showed the characteristic absorptions of imide and ester groups around

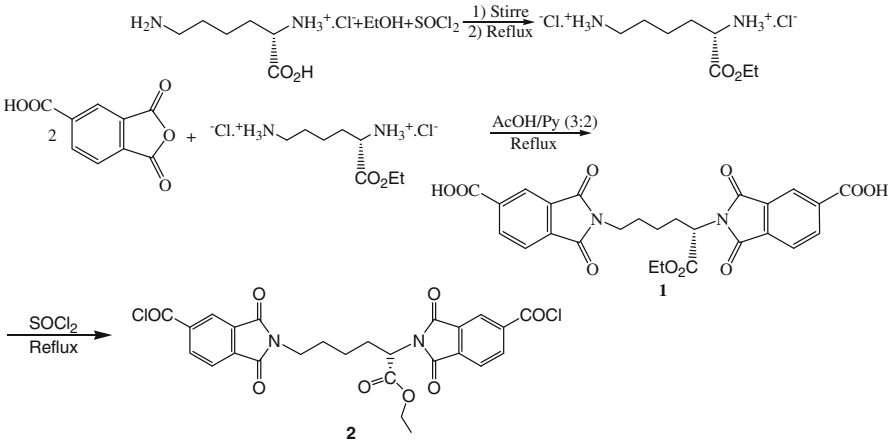


**Scheme 1** Synthesis of ethyl L-lysine-N,N′-ditrimellitoyl diacylchloride

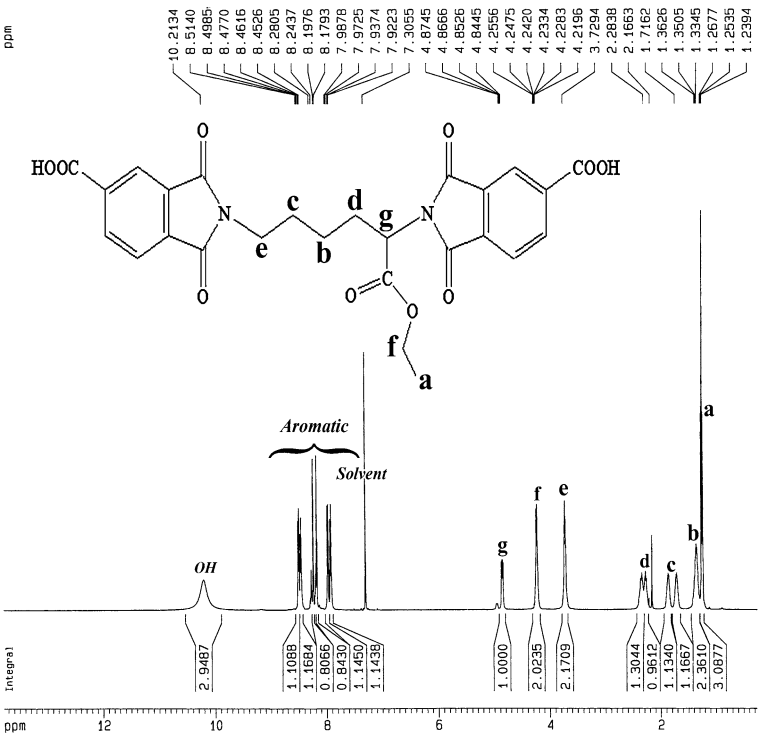


**Fig. 1** $^{1}$H NMR spectrum of diacid **1**

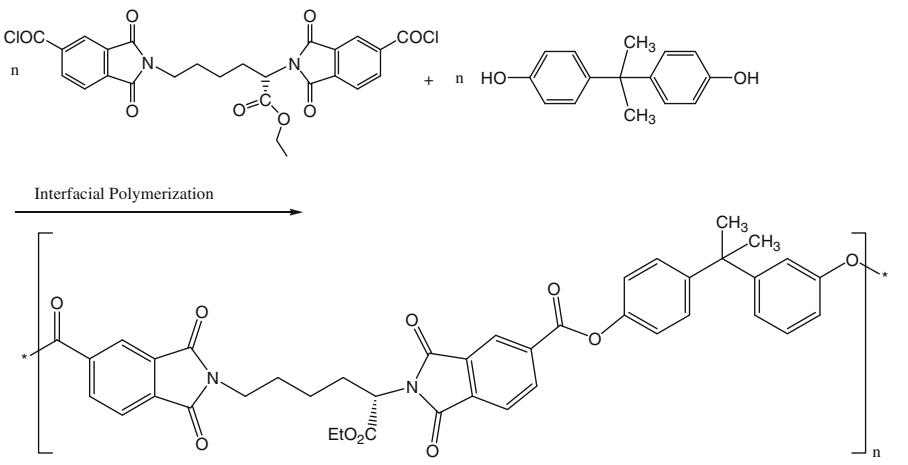


**Scheme 2** Interfacial polymerization

1760 and 1720 cm$^{-1}$, which are related to carbonyls stretching of imide and ester groups, respectively. The peaks at 1387 and 727 cm$^{-1}$ show the existence of the imide heterocycle in this polymer. FT–IR spectrum of PEI/12$CH_3$-MMT (5 wt%) is

shown in Fig. 2, where the characteristic peaks of pure PEI and MMT are still maintained, it may be proved that the structure of PEI was affected by the presence of MMT.

In the presence of the non-coplanar and twisted units into the backbone of this PEI decreased the intermolecular forces between the polymer chains and reduced the crystallinity of this polymer. The XRD experiments were used for measuring the interlayer distance of MMT after modification with the ammonium salt and in nanocomposites (Fig. 3). The main peak in the diffraction pattern of the $12CH_3$-MMT reference standard ($2\theta \sim 6.0^\circ$) was attributed to the formation of the interlayer spaces by insertion of ammonium salt along the [001] direction. The interlayer distance estimated from the $2\theta$ value was 14.70 Å. The [001] peaks for the solid product recovered from PEI/$12CH_3$-MMT (20 wt%) was measured at $2\theta \sim 5.8°$ and 9.1°, i.e., the interlayer distances were 15.22 and 9.70 Å. For PEI/$12CH_3$-MMT (10 wt%) product that was measured at $2\theta \sim 5.6^\circ$ and $9.0^\circ$, i.e., the interlayer distances were 15.76 and 9.81 Å and For PEI/$12CH_3$-MMT (5 wt%) product that was measured at $2\theta \sim 5.5^\circ$ and $10.0^\circ$, i.e., the interlayer distances were 16.05 and 8.83 Å. The increases in interlayer distance were interpreted as due to the segregation and adsorption of the PEI molecules into the interlayer spaces. The XRD data of PEI/$12CH_3$-MMT nanocomposites indicated a degree of exfoliation. PEI/$12CH_3$-MMT (5%) showed a degree of exfoliation, PEI/$12CH_3$-MMT (10%) shows a degree of flocculated and PEI/$12CH_3$-MMT (20%) shows some intercalated structure. So, the clay content of an exfoliated nanocomposite is much lower than that of an intercalated nanocomposite. In intercalated

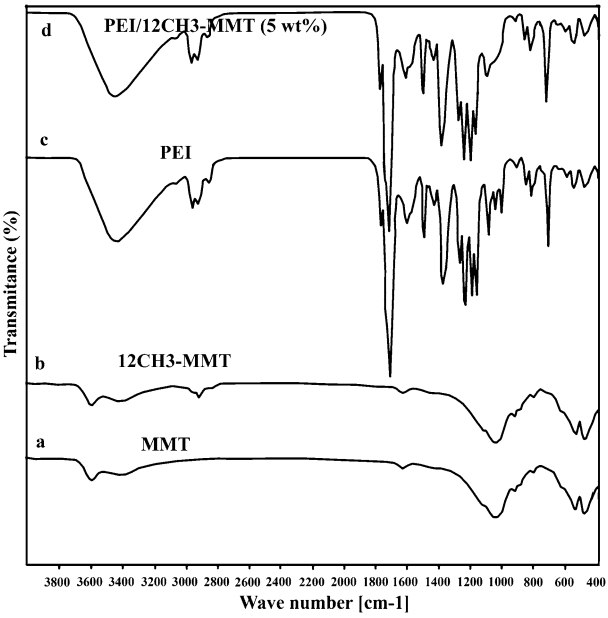


**Fig. 2** FT–IR spectra of *a* pure MMT, *b* $12CH_3$-MMT, *c* pure PEI, *d* PEI/$12CH_3$-MMT (5 wt%)

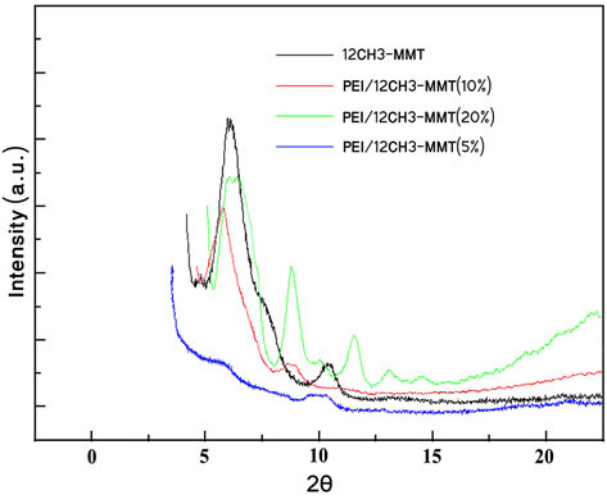


**Fig. 3** XRD curves of $12CH_3$-MMT and nanocomposites of PEI/$12CH_3$-MMT

nanocomposites, the insertion of a polymer matrix into the layered silicate structure occurs in a crystallographically regular fashion. Intercalated nanocomposites are normally interlayer by a few molecular layers of polymer. In flocculated nanocomposites silicate layers are some times flocculated due to hydroxylated edge–edge interaction of the silicate layers. In exfoliated nanocomposites the individual clay layers are separated in a continuous polymer matrix by an average distances that depends on clay loading.

The level and degree of dispersion was investigated by TEM using an acceleration voltage of 80 kV and samples of approximately 60 nm were microtomed at room temperature and transferred to carbon-film-coated Cu grids. TEM allows a qualitative understanding of the internal structure, spatial distribution of the various phases, and views of the defect structure through direct visualization, but it is time-intensive. Figure 4 shows the TEM micrograph of PEI/$12CH_3$-MMT (5 wt%) nanocomposite in 100 nm scale. Well-dispersed organo-modified MMT in PEI matrix are observed obviously. This image exhibited a mixed morphology. Among individual silicate layers, only part of them were intercalated in the poly(ester-imide) matrices, whereas the remnant displayed aggregated phenomenon. Apart from that, the aggregated phenomenon is possibly due to the number of poly(ester-imide) chains that is not large enough to resist the attraction between silicate interlayers. Furthermore, the poly(ester-imide) chains perhaps possessed the lying down conformation as they were slightly inserted into space between interlayer silicates. When the content of clay decreased (5%), plenty of poly(ester-imide) chains would develop into an extended morphology and eventually form an exfoliated conformation.

The thermal properties of the PEI and PEI/$12CH_3$-MMT nanocomposites were evaluated by TGA at a heating rate of 10 °C/min, under a nitrogen atmosphere (Fig. 5). Table 1 shows the data for the thermal degradation of the PEI and its

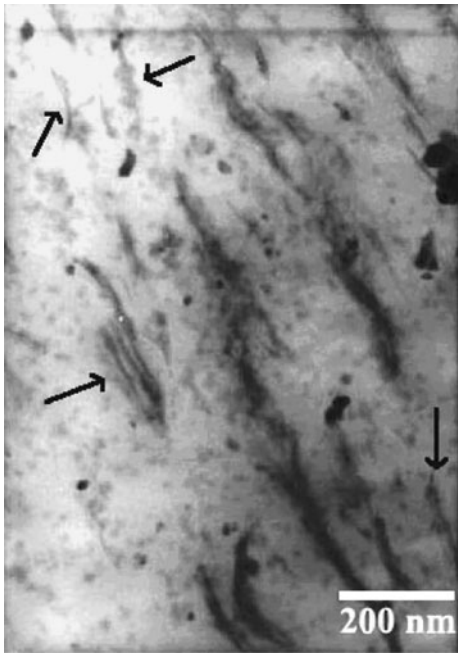


**Fig. 4** TEM micrograph of PEI/12$CH_3$-MMT (5 wt%); *arrows* indicates exfoliated clay

nanocomposites, including the temperature at which 10% degradation occurs (T10), char yield at 600 °C and also limiting oxygen index (LOI) [16].

$$\text{LOI} = 17.5 + 0.4\text{CR}, \text{ where CR} = \text{Char yield}$$

PEI had a high decomposition temperature of about 322 °C, which was further improved when 12$CH_3$-MMT was introduced. Incorporation of inorganic nanoparticles in polymer matrix improves its thermal stability. Increasing in the thermal stability may be due to the high thermal stability of 12$CH_3$-MMT network or by acting as a superior insulator and mass transport barrier to the volatile products generated during decomposition. The char yield of pure PEI at 600 °C is 17.6%, while those of the nanocomposites (PEI/12$CH_3$-MMT 5, 10, 20 wt%) at 600 °C are in the range of 22.4-41.5%, they were enhanced with an increase of 12$CH_3$-MMT content in the PEI. The high weight residue of the PEI can be arisen from the participation of thermally stable aromatic rings and imide group in its repeating unit.

## Conclusions

In this study, a novel thermally stable and optically active PEI was successfully prepared by interfacial polycondensation method. The polymerization was carried out by the reaction of natural L-lysine-based diacyl chloride (**2**) with aromatic bis phenol A. The prepared PEI is thermally stable and soluble in common organic solvents. Novel PEI/12$CH_3$-MMT nanocomposites were synthesized by ultrasonic method as a simple and inexpensive route to prepare the polymer/nanocomposites,

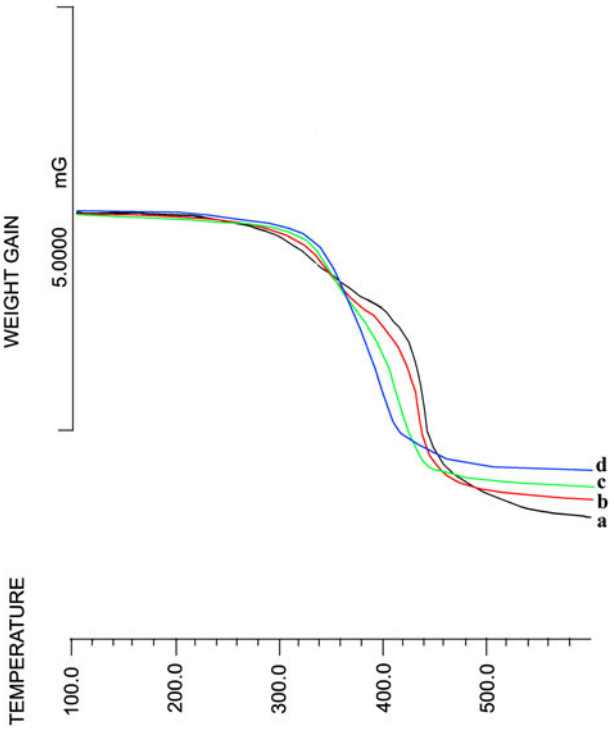


**Fig. 5** TGA thermograms of PEI (*a*), PEI/12$CH_3$-MMT (5 wt%) (*b*), PEI/12$CH_3$-MMT (10 wt%) (*c*), PEI/12$CH_3$-MMT (20 wt%) (*d*) bionanocomposites under a nitrogen atmosphere at heating rate of 10 °C/min

**Table 1** Thermal properties of the PEI and PEI/12$CH_3$-MMT bionanocomposites

| Polymer | $T_{10\%}$[a] | Char yield (%)[b] | LOI[c] |
|---|---|---|---|
| PEI | 322 | 17.6 | 24.5 |
| PEI/12$CH_3$-MMT (5 wt%) | 338 | 22.4 | 26.5 |
| PEI/12$CH_3$-MMT (10 wt%) | 341 | 33.7 | 31.0 |
| PEI/12$CH_3$-MMT (20 wt%) | 350 | 41.5 | 46.1 |

[a] Temperature at which 10% weight loss was recorded by TGA at heating rate of 10 °C/min under a nitrogen atmosphere

[b] Weight percentage of material left after TGA analysis at a temperature of 600 °C under a nitrogen atmosphere

[c] Limiting oxygen index (LOI) evaluating char yield at 600 °C

using MMT modified by ammonium salt of dodecyl amine. The modification would make the MMT scatter within the matrix more homogeneously. Moreover, the final mechanical properties could be greatly improved. Morphology study of resulting nanocomposites showed well-dispersed 12$CH_3$-MMT in the polymer matrix by TEM analyses. TGA studies indicated that thermal stability of the nanocomposites

has enhanced with increasing $12CH_3$-MMT content. FT–IR and XRD data also confirmed that $12CH_3$-MMT is dispersed in the PEI matrix. Since this PEI has amino acid in its polymer architecture, it could be categorized under environmentally benign polymers and could be composted with organic wastes and recycled to enrich the soil. Also, it has the potential to be used as optically active packing materials in column chromatography for the resolution of racemic mixtures. Polymers that are synthesized from naturally occurring building blocks such as amino acids are favorable materials for pharmaceutical and biomedical purposes since their degradation products are nontoxic and can be metabolized correctly by alive tissues. Combining nanosized bioactive materials with biopolymer could produce materials with greater bioactivity. Therefore, having both natural amino acid and $12CH_3$-MMT in these novel nanocomposites it would be suitable to name them as bionanocomposites polymers which may be anticipated to have biodegradability and biocompatibility properties.

**Acknowledgment** We gratefully acknowledge the funding support received for this project from the Payame Noor University (PNU).

## References

1. Vandermeulen GWM, Klok HA (2004) Peptide/protein hybrid materials: enhanced control of structure and synthetic polymers. Macromol Biosci 4:383–398
2. Majo MA, Alla A, Bou JJ, Herranz C, Munoz-Guerra S (2004) Synthesis and characterization of polyamides obtained from tartaric acid and L-lysine. Euro Polym J 40:2699–2708
3. Liaw DJ, Fan CL, Lin CC, Wang KL (2004) Synthesis and characterization of new soluble poly(ester-imide)s containing noncoplanar 2,2′-dimethyl-4,4′-biphenylene unit. J Appl Polym Sci 92:2486–2493
4. Liu T, Burger C, Chu B (2003) Nanofabrication in polymer matrices. Prog Polym Sci 28:5–26
5. Ishizu K, Tsubaki K, Mori A, Uchida S (2003) Architecture of nanostructured polymers. Prog Polym Sci 28:27–54
6. Rozenberg BA, Tenne R (2008) Polymer-assisted fabrication of nanoparticles and nanocomposites. Prog Polym Sci 33:40–112
7. Ray SS, Okamoto M (2003) Polymer/layered silicate nanocomposites: a review from preparation to processing. Prog Polym Sci 28:1539–1641
8. Mehta GK, Mark J, Lee JW et al (2007) Polyelectrolyte-clay-protein layer films on microfluidic PDMS bioreactor surfaces for primary murine bone marrow culture. Adv Funct Mater 17:2701–2709
9. Liang ZM, Yin J, Xu HJ (2003) Polyimide/montmorillonite nanocomposites based on thermally stable, rigid-rod aromatic amine modifiers. Polymer 44:1391–1399
10. Imai Y, Nishimura S, Abe E et al (2002) High-modulus poly(ethylene terephthalate)/expandable fluorine mica nanocomposites with a novel reactive compatibilizer. Chem Mater 14:477–479
11. Kim J, Ahmed R, Lee SJ (2001) Synthesis and linear viscoelastic behavior of poly(amic acid)–organoclay hybrid. J Appl Polym Sci 80:592–603
12. Burnside SD, Giannelis EP (1995) Synthesis and properties of new poly(dimethylsiloxane) nanocomposites. Chem Mater 7:1597–1600
13. Mallakpour S, Soltanian S (2010) Studies on syntheses and morphology characteristic of chiral novel poly (ester-imide)/$TiO_2$ bionanocomposites derived from L-phenylalanine based diacid. Polymer 51:5369–5376
14. Zahmatkesh S, Hajipour AR (2009) Microwave-assisted synthesis and characterization of some optically active poly (ester-imide) thermoplastic elastomers. e-Polymers 068
15. Mallakpour S, Dinari M (2011) Preparation and characterization of new organoclays using natural amino acids and Cloisite $Na^+$. Appl Clay Sci. doi:10.1016/j.clay.2010.12.028
16. Van Krevelen DW, Hoftyzer PJ (1976) Properties of polymers, 3rd edn. Elsevier, Amsterdam